Response of streamflow to multiple earthquakes

Michael Manga

Department of Earth and Planetary Science, University of California, Berkeley, California, USA
Earth Sciences Division, Lawrence Berkeley National Laboratory, Livermore, California, USA

Emily E. Brodsky

Department of Earth and Space Sciences, University of California, Los Angeles, California, USA

Michael Boone

Department of Earth and Planetary Science, University of California, Berkeley, California, USA
Earth Sciences Division, Lawrence Berkeley National Laboratory, Livermore, California, USA

[1] We analyze the streamflow response of Sespe Creek, CA, to several large earthquakes. We find that flow increased after three earthquakes, and that the observed changes in flow have the same character. Both those earthquakes that induced static extension and those that induced static contraction cause flow to increase; streamflow thus appears to respond to dynamic strain. We find that all postseismic responses can be explained by a model in which pore pressure increases coseismically without any changes in hydraulic diffusivity. There is a particle velocity threshold in the range of $5-20$ cm/s to induce the pore pressure increase. *INDEX TERMS:* 7212 Seismology: Earthquake ground motions and engineering; 1829 Hydrology: Groundwater hydrology; 1860 Hydrology: Runoff and streamflow; 5104 Physical Properties of Rocks: Fracture and flow; *KEYWORDS:* streamflow, earthquakes, consolidation, pore pressure, liquefaction. **Citation:** Manga, M., E. E. Brodsky, and M. Boone, Response of streamflow to multiple earthquakes, *Geophys. Res. Lett.*, *30*(5), 1214, doi:10.1029/2002GL016618, 2003.

1. Introduction

[2] One common hydrologic response to earthquakes is an increase in stream discharge. Discharge increases appear to be coseismic, typically peaking within a few days to weeks after the earthquake. Changes in streamflow are usually attributed to either enhanced hydraulic conductivity [e.g., *Rojstaczer and Wolf*, 1992; *Sato et al.*, 2000] or release of water from storage [e.g., *Muir-Wood and King*, 1993].

[3] Here we analyze the response of Sespe Creek, California, to multiple earthquakes in order to test conceptual models for the origin of increased streamflow. Our analysis is made possible because of the availability of long, continuous gauging measurements collected by the USGS (1928-present) and the relatively high rate of seismicity in California. Our study thus complements the more numerous studies that focus on the response of a set of streams to a given earthquake [e.g., *Rojstaczer and Wolf*, 1992; *Muir-Wood and King*, 1993; *Sato et al.*, 2000; *Montgomery et al.*, 2003]. The studies of *King et al.* [1994] and *Leonardi et al.* [1990] also address the response of discharge (in both cases springs) to several earthquakes.

2. Setting

[4] The Sespe Creek watershed is located in the Transverse Ranges. Most of the 650 km^2 gauged basin (USGS gauging station 11113000) lies within the Santa Lucia wilderness area. The subsurface geology consists of consolidated Neogene marine and non-marine sedimentary deposits. Quaternary, unconsolidated alluvial deposits usually lie adjacent to the stream. Figure 1 shows the location of the basin and the nearest precipitation station (Ventura, CA) with continuous records that span the range of dates for which we have both streamflow data and large earthquakes.

3. Streamflow Model

[5] Consider a one-dimensional confined aquifer extending from position $x = 0$ to $x = L$ (the stream). Evolution of head in the aquifer is governed by the diffusion equation

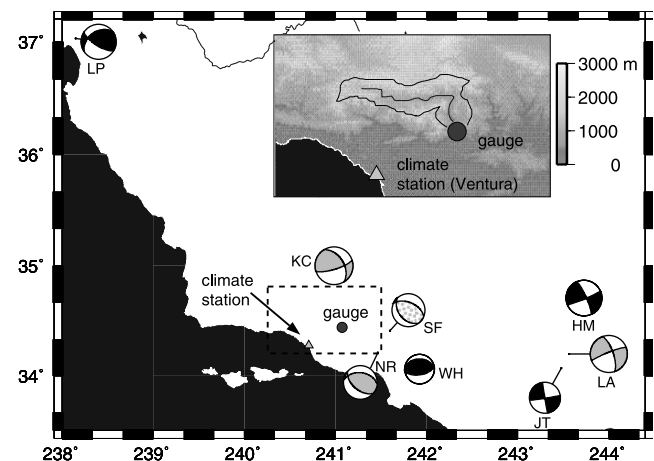$$\frac{\partial h}{\partial t} = D \frac{\partial^2 h}{\partial x^2}, \qquad (1)$$

Figure 1. Map of southern California showing the location and focal mechanisms of large earthquakes (grey - streamflow increase, grey dots - possible increase, black - no change), the Sespe Creek basin, the location of the gauge, and the location of the climate station in Ventura. Inset shows the region in the dashed box.
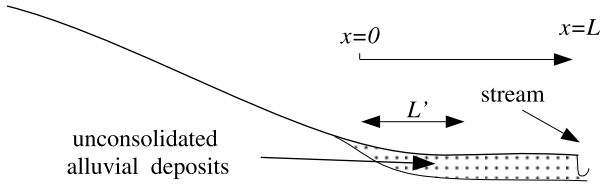
Figure 2. Schematic illustration of the model geometry.

where D is hydraulic diffusivity. For a confined aquifer $D = K/S_s$, where K is the horizontal hydraulic conductivity, and S_s is the specific storage. Discharge q into the stream at $x = L$ is given by

$$q = -AK\partial h/\partial x \qquad (2)$$

where A is the vertical cross-sectional area (aquifer thickness b times the length of the stream). Equation (1) is also the linearized form of the Boussinesq equation that describes flow in an unconfined aquifer, but with $D = bK/S_y$, where S_y is the specific yield.

[6] For sufficiently long times after recharge, the solutions to equations (1)–(2) predict that

$$\frac{d \log q}{dt} = -\pi^2 D/4L^2. \qquad (3)$$

Equation (3) describes what is often called baseflow recession [e.g., *Domenico and Schwartz*, 1998] and, during periods without precipitation, is consistent with the decrease in discharge in Sespe Creek for $D/L^2 = 1.4 \times 10^{-7} \text{ s}^{-1}$ [*Manga*, 2001]. If we assume baseflow is dominated by the unconsolidated sandy alluvial deposits in the flood plain (Figure 2), and choose reasonable values of $K = 4 \times 10^{-5}$ m/s, $S_y = 0.4$ and $b = 5$ m, this recession rate implies $L \approx 60$ m, the typical horizontal extent of the flood plain.

[7] At time of the earthquake, $t = 0$, we assume that head increases an amount h_0 in the region $0 < x < L'$. Because the diffusion equation is linear, we can superimpose the additional streamflow induced by the earthquake on the baseflow recession described by equation (3). The excess discharge, q_{EQ}, at time t after the earthquake is given by [e.g., *Roeloffs*, 1998]

$$q_{EQ} = \frac{4KAh_0}{L} \sum_{n=0}^{\infty} (-1)^n \cos\left(\frac{(2n+1)\pi L'}{4L}\right)$$

$$\cdot \sin\left(\frac{(2n+1)\pi L'}{4L}\right) \cdot \exp\left(-\frac{(2n+1)^2 \pi^2 D}{4L^2}t\right). \qquad (4)$$

The total excess discharge Q_{EQ} is then given by

$$Q_{EQ} = \int_{t=0}^{\infty} q_{EQ}dt. \qquad (5)$$

[8] The model in equations (4)–(5) does not specify the mechanism for the head increase; it only models the evolution of head once the increase in head has occurred. In the case of a successful fit, we can extend the analysis and constrain the mechanism for the head change by using the static and dynamic strains generated by the earthquake to predict, 1) the sign of the head change h_0 (Section 4), 2) the threshold for generating observable stream flow changes (Section 5), and 3) the magnitude of h_0 (Section 6).

4. Observations and Model Results

[9] We analyzed the response of streamflow to 48 earthquakes with moment magnitudes greater than 5.0. Figure 1 shows the location and focal mechanisms of some of the larger earthquakes; Table 1 lists the properties of these earthquakes and the stream response. Three earthquakes induced clear postseismic changes; the response to the San Fernando earthquake is complicated by a small amount of precipitation (a few mm) that might influence streamflow. The upper bound on the inferred head changes for the San Fernando earthquake assumes that the small amount of precipitation had no effect on discharge. The static coseismic strain in the drainage basin is computed using COU-LOMB2.2 [*Toda et al.*, 1998]. The particle velocity in the basin (at the stream gauge) is computed for each earthquake using a discrete wavenumber method to synthesize Green's functions [*Bouchon*, 1979; *Zhu and Rivera*, 2002] with a standard 1-dimensional Southern California velocity model. A comparison of the computed ground velocities with those measured at nearby strong-motion stations Moorpark and Piru for the San Fernando, Whittier and Northridge earthquakes indicates that the computed velocities are accurate to within a factor of two.

[10] Streamflow increases occur for earthquakes that cause both static extension (Northridge and possibly San Fernando) and contraction (Kern County, Landers) in the basin. Thus the increased discharge is not caused by increases in pore pressure induced by the coseismic static strain, as suggested by *Muir-Wood and King* [1993]. Rather, streamflow changes in Sespe Creek must be caused by dynamic strain releasing water from storage.

[11] Figure 3 shows measured discharge (circles) and model predictions (curves) from equation (4) for the four

Table 1. Earthquake and Stream Response Data

Earthquake Magnitude (Mw)	Date (day/mo/yr)	Distance (km)	Static Strain[a]	Horizontal and Velocity[b] (cm/s)	Normalized Head Change[c] $4KAh_0/L$ (m³/s)	pre-EQ Discharge (m³/s)	Rainfall Equivalent[c] (mm)
Kern County (KC), 7.5	21/07/52	63	C	64.9	2.6 ± 0.3	0.086	2.8 ± 0.3
Northridge (NR), 6.7	17/01/94	44	E	14.9	3.1 ± 0.3	0.51	3.4 ± 0.3
Landers (LA), 7.3	28/06/92	230	C	8.1	1.2 ± 0.1	0.82	1.3 ± 0.1
San Fernando (SF), 6.6	9/02/71	48	E	27.0	0.3 ± 0.3	1.9	0.3 ± 0.3
Hector Mine (HM), 7.1	10/10/99	245	C	10.0	-	0.013	-
Whittier (WH), 5.9	1/10/87	89	-	4.1	-	0.14	-
Loma Prieta (LP), 6.9	17/10/89	390	E	1.7	-	0.028	-
Joshua Tree (JT), 6.1	23/04/92	225	C	2.0	-	4.8	-

[a]Contraction (C), extension (E), or near the nodal plane (-).
[b]Calculated. Uncertainty is estimated to be a factor of 2.
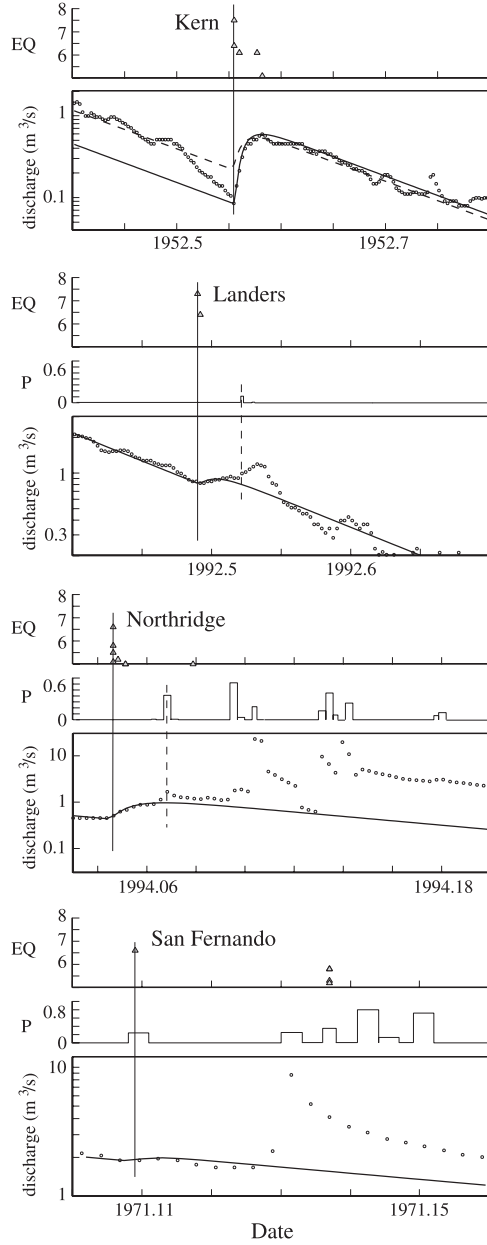[c]Uncertainty reflects range of possible model fits in Figure 3

Figure 3. Response of streamflow to the a) Kern County, b) Landers, c) Northridge, and d) San Fernando earthquakes. In each set of three panels, the top curve shows the magnitude and time of earthquakes, the middle panel shows precipitation (P) at Ventura, CA (see Figure 1), and the bottom panel shows measured (black circles) and modeled (continuous curves) discharge. Note different time axes. For Kern County, there was no precipitation, and the solid and dashed curves indicate models with the largest and smallest head changes that are considered reasonable fits to the data. See Table 1 for uncertainties.

streams with possible postseismic responses: Northridge, Kern County, Landers and San Fernando. For all four earthquakes, we use the model described by equation (4) to determine the normalized head change (the factor $4KAh_0/L$ in equation 4); we assume $L'/L = 0.4$ and use $D/L^2 = 1.4 \times 10^{-7}$ s^{-1} from the recession flow analysis [*Manga*, 2001]. The model predictions are in good agreement with meas-

ured discharge, at least until discharge is influenced by precipitation.

[12] For the Kern County earthquake, the model captures two distinctive features of the postseismic response: 1) the rate of increase of discharge (peak discharge occurs several days after the earthquakes), and 2) the return of streamflow to the pre-earthquake recession rate. That is, although stream discharge q may increase rapidly, baseflow recession $d \log q/dt$ is unchanged after the earthquake suggesting that the (horizontal) hydraulic conductivity of the groundwater system providing baseflow does not change. Multiple processes can cause changes in streamflow, and the dominant processes might be expected to vary between regions. Nevertheless, for regional earthquakes (more than 1 fault length, but less than tens of fault lengths, away from the epicenter) equation (2) shows that if K does not change (inferred from the fact that D does not change) then the head gradient $\partial h/\partial x$ must change. Closer to the epicenter, discharge changes appear to be correlated with the pattern of static strain [e.g., *Lee et al.*, 2002] and may respond to change in fault zone permeability [e.g., *Leonardi et al.*, 1990].

4.1. Dynamic Strain Threshold

[13] Figure 4 shows the modeled coseismic increase in head (determined as the ratio $4KAh_0/L$) as a function of the calculated amplitude of horizontal velocity V_H in the basin (dynamic strain is proportional to velocity). We plot V_H on the abscissa because the shear stresses that cause permanent changes in pore space, such as those that result in consolidation and liquefaction, are dominated by horizontal motions [*Terzaghi et al.*, 1996, p. 197]. Although we have only 3 (possibly 4) examples of increased discharge, there appears to be a velocity threshold to induce streamflow changes in the range 5–20 cm/s.

[14] The nonmonotonic responses shown in Figure 4 may reflect two sets of complications. First, unmodeled variability in the site, directivity, and basin effects may influence the velocity. Second, if the excess water is generated at shallow depths, the amount of water released may then also
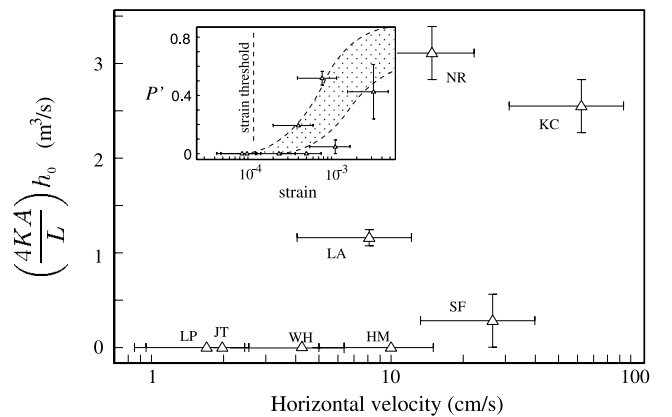

Figure 4. Relationship between calculated amplitude of horizontal velocity and normalized head changes inferred from the model fits in Figure 3. Inset: Pore pressure ratio, P', as a function of strain - see text for details. The stippled region indicates the range of experimental data [after *Vucetic*, 1994].

depend on water level and degree of saturation. The response to Northridge lends some support to this hypothesis - Northridge induced a larger head increase, h_0, even though the dynamic strain was smaller than that for Kern County. Head in the groundwater system prior to Northridge (Table 1), however, was larger (discharge increases as head increases) and the water level would also have been higher.

4.2. Mechanism?

[15] One mechanism for rapidly releasing water from storage by dynamic straining is shear-induced consolidation of alluvial deposits (Figure 2). Cyclic loading of unconsolidated materials, for example by seismic waves, can rearrange grains into a closer packing. The reduction of pore volume increases pore pressure. The change in porosity, however, will also be so small that there may be no detectable changes in D. In detail, if $K \propto \phi^3$ [e.g., *Domenico and Schwartz*, 1998] where ϕ is porosity, and $S_y \approx \phi$ for unconsolidated sediments, then $D \propto \phi^2$ and $dD/D = 2d\phi/\phi$; thus, if ϕ changes 5% then D changes by 10%, a change that is difficult to detect [*Manga*, 2001].

[16] *Dobry et al.* [1982] summarize experimental studies of pore pressure changes in sands induced by cyclic loading. Two general conclusions can be drawn from these laboratory measurements. First, there is a threshold strain amplitude, typically on the order of 10^{-4}, that is not sensitive to confining stress, fabric, or porosity [*Vucetic*, 1994]. Second, for shear strains greater than the threshold, the pore pressure ratio P' (generated pore pressure divided by the effective pressure σ') is most sensitive to the strain amplitude.

[17] The inset of Figure 4 compares the measurements compiled in *Dobry et al.* [1982] with our inferred pressure changes. The number of cycles is of secondary importance in Figure 4 because of the nonlinear response. We estimate the strain amplitude by dividing the calculated particle velocity by the shear velocity of the materials being consolidated (assumed to be 200 m/s). To calculate P' we assume, as in section 2, $K = 4 \times 10^{-5}$ m/s, $A/L = 25$ km, and $\sigma' = 2 \times 10^4$ Pa, while acknowledging that these values are highly uncertain and spatially variable. Nevertheless, with these plausible estimates we find good agreement with the predicted strain threshold and reasonable agreement between the magnitude of h_0 and the laboratory pore pressure changes.

[18] The volume of excess discharge, expressed as $R = Q_{EQ}$/basin area (rainfall equivalent in Table 1), provides a constraint on the amount of consolidation. If consolidation occurs in the alluvial deposits, say a fraction $f \approx 0.01$ of the basin, then the subsidence R/f can exceed a few tens of cm (the values assumed in Figure 4 predict h_o up to 80 cm and hence subsidence ϕh_o up to 30 cm). Future geodetic studies can potentially identify the location and magnitude of any subsidence and hence distinguish between mechanisms.

5. Summary

[19] Although the limited occurrences of increased streamflow hamper our ability to understand their origin, the available data for Sespe Creek provide three constraints. First, dynamic strain, rather than static strain, is responsible for the changes in discharge. Second, the measured hydrographs are consistent with the hydraulic conductivity of the aquifer providing baseflow remaining unchanged. Instead, pore pressure increases within the aquifer that provides base flow. Third, there appears to be a dynamic strain threshold which is consistent with consolidation increasing pore pressures.

References

Bouchon, M., Discrete wave number representation of elastic wave field in three-space dimension, *J. Geophys. Res.*, *84*, 3609–3614, 1979.

Dobry, R., R. S. Ladd, F. Y. Yokel, R. M. Chung, and D. Powell, Prediction of pore water pressure buildup and liquefaction of sands during earthquakes by the cyclic strain method, *NBS Building Sci. Ser. U. S.*, *138*, 1982.

Domenico, P. A., and F. W. Schwartz, *Physical and Chemical Hydrogeology*, 2nd ed., John Wiley, New York, 1998.

King, C. Y., D. Basler, T. S. Presser, W. C. Evans, L. D. White, and A. Minissale, In search of earthquake-related hydrologic and chemical changes along Hayward fault, *Appl. Geochem.*, *9*, 83–91, 1994.

Lee, M., T.-K. Liu, K.-F. Ma, and Y.-M. Chang, Coseismic hydrological changes associated with dislocation of the September 21, 1999 Chichi earthquake, Taiwan, *Geophys. Res. Lett.*, *29*(17), 1824, doi:10.1029/2002GL015116, 2002.

Leonardi, V., F. Arthaud, A. Tovmassian, and A. Karakhanian, Tectonic and seismic conditions for changes in spring discharge along the Garni right lateral strike slip fault (Armenian Upland), *Geodin. Acta*, *11*, 85–103, 1990.

Manga, M., Origin of postseismic streamflow changes inferred from baseflow recession and magnitude-distance relations, *Geophys. Res. Lett.*, *28*, 2133–2136, 2001.

Montgomery, D. R., H. M. Greenberg, and D. T. Smith, Streamflow response to the Nisqually earthquakes, *Earth Planet Sci. Lett.*, in press, 2003.

Muir-Wood, R., and G. C. P. King, Hydrological signatures of earthquake strain, *J. Geophys. Res.*, *98*, 22,035–22,068, 1993.

Roeloffs, E. A., Persistent water level changes in a well near Parkfield, CA, due to local and distant earthquakes, *J. Geophys. Res.*, *103*, 869–889, 1998.

Rojstaczer, S., and S. Wolf, Permeability changes associated with large earthquakes: An example from Loma Prieta, California, *Geology*, *20*, 211–214, 1992.

Sato, T., R. Sakai, K. Furuya, and T. Kodama, Coseismic spring flow changes associated with the 1995 Kobe earthquake, *Geophys. Res. Lett.*, *27*, 1219–1222, 2000.

Terzaghi, K., R. B. Peck, and G. Mesri, Soil Mechanics in engineering practice, 3rd ed., John Wiley, New York, 1996.

Toda, S., et al., Stress transferred by the 1995 M − w = 6.9 Kobe, Japan, shock: Effect on aftershocks and future earthquake probabilities, *Geophys. Res. Lett.*, *103*, 24,543–24,565, 1998.

Vucetic, M., Cyclic threshold shear strains in soils, *J. Geotech. Eng.*, *120*, 2208–2228, 1994.

Zhu, L., and L. A. Rivera, A note on the dynamic and static displacements from a point source in multilayered media, *Geophys. J. Int.*, *148*, 69–627, 2002.

_____

M. Boone and M. Manga, Department of Earth and Planetary Science, University of California, Berkeley, CA 94720, USA. (manga@seismo.berkeley.edu)

E. E. Brodsky, Department of Earth and Space Sciences, University of California, Los Angeles, CA 90095, USA. (brodsky@ess.ucla.edu)